Propagation and Severity of Coal-Dust Explosions and the Effect of Radiation in Different Channel Lengths

Swagnik Guhathakurta[1,2]; Ryan W. Houim[2]
[1]Eindhoven University of Technology, Eindhoven, North Brabant, Netherlands
[2]University of Florida, Gainesville, Florida, U.S.A

1 Introduction

There is significant interest in multiphase reacting flows due to practical applications including propulsion, cleaner alternative fuels, and explosion safety. Numerical studies of these multiphase reactive flows often neglect radiation heat transfer due its inherent complexity and computational cost. In cases, where it is considered, an optically thick assumption is usually made. In most cases, however, the medium is neither optically thick nor thin, but in an intermediate regime. In these scenarios, the only option is to solve the radiation transfer equation (RTE) without such approximations.

Despite its vast importance, the understanding of dust flames and explosions remains underdeveloped. To some extent, this is due to the challenges of conducting experiments with a laminar suspension of solid particles, which is required to characterize parameters that affect the burning velocity. Experimental mines such as Barbara in Poland and the Bruceton Experimental Mine in the USA have been used to study dust explosions at mining scales. Most lab-scale data available on the combustion of dust clouds are obtained from experiments using closed bomb vessels. These experiments usually do not provide visual access and typically measure only pressure within the vessel. While the pressure time history provides important information on the explosivity of dust clouds, fundamental knowledge on the propagation mechanism and structure of dust flames are not obtained. Given the challenges of experiments, computational fluid dynamics (CFD) simulations are necessary to understand the complex behavior of dust flame propagation.

In our previous work [1, 2], we explained two-dimensional simulations of layered coal-dust explosions assuming gray radiation. Results showed that radiation can have significant influence on important flame parameters such as the flame temperature, flame speed, and flame propagation behaviour of layered dust explosions. Radiation was observed to have opposite effects depending on the scenario. In some cases radiation enhanced the explosion propagation while in others, it slowed the propagation, or in extreme cases even quenched the flame.

2 Problem Description and Numerical Models

Figure 1 shows the numerical setup that is used in this study. The computational domain is a long and narrow channel. Both ends of the channel are closed and are considered cold (300 K) and black. The top

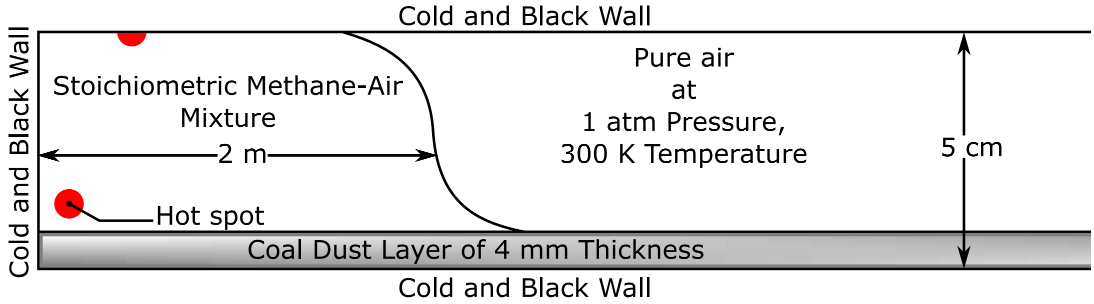

Figure 1: Initial and boundary conditions of the numerical setup.

and bottom boundaries are symmetry planes that are also cold and black. The height of the channel is 5 cm and two channel lengths of 10 m and 40 m are considered. There is a 4 mm-thick layer of coal-dust on the floor of the channel with a volume fraction of 47%. Near the left closed boundary, there are two "hot spots", which are high temperature and pressure regions with an unreacted stoichiometric mixture of methane and air. The first 2 m of the channel is filled with this same mixture which is then gradually transitioned into pure air over the next 1 m. The "hot spots" trigger a detonation near the left boundary, which mimics a "primary explosion" in coal mines.

The coal particles are assumed to be spherical and monodisperse with 30 μm diameter (which have the highest explosibility) [3], assumed to have a constant specific heat capacity of 987 J/kg.K, and a material density, ρ_s, of 1200 kg/m^3 [4]. The composition by mass of the coal particles is 93% dry ash-free carbon, 6% ash and 1% moisture.

The full set of coupled, multiphase, compressible, unsteady Navier Stokes equations along with the Radiative Transport Equations (RTE) are solved using an in-house code, HyBurn. The solid phase governing equations are based on a kinetic-theory approach with Eulerian framework. The complete equation set and numerical modelling approached are given in [5,6]. The solid phase model accounts for drag, convective heat transfer, particle-particle interactions and inelastic collisions. High order Godunov methods are used to solve the resulting governing equations.

The radiation field is obtained by solving the RTE with a third-order filtered spherical harmonics approximation (FP_3) [7]. We assume gray radiation and isotropic scattering to simplify the model and reduce the computational cost. The gray Planck-mean extinction coefficients for the different gas-phase species (CH_4, O_2, CO_2, CO and H_2O) are calculated from curve fits to the data from the RADCAL program [8]. The Planck-mean extinction and scattering coefficients for the solid-phase coal particles are obtained from the Buckius and Hwang correlation [9].

The gas-phase methane-air reaction mechanism is a two-step reaction mechanism, which is an Arrhenius reaction based on the BFER reaction mechanism [10] from CERFACS. The gas-phase species are CH_4, O_2, CO_2 and H_2O, and CO. The coal volatiles are approximated as methane and the devolatilization rate is described using a Kobayashi model [11]. The devolatilization process releases gaseous methane and leaves behind solid carbon (char), which undergoes reaction with oxygen at the surface of the particles via a combination of kinetic and diffusion limited processes [12]. Finally, the trapped moisture evaporates and forms gaseous water vapour [13]. Details of the solid-phase reaction mechanisms can be found in [1].

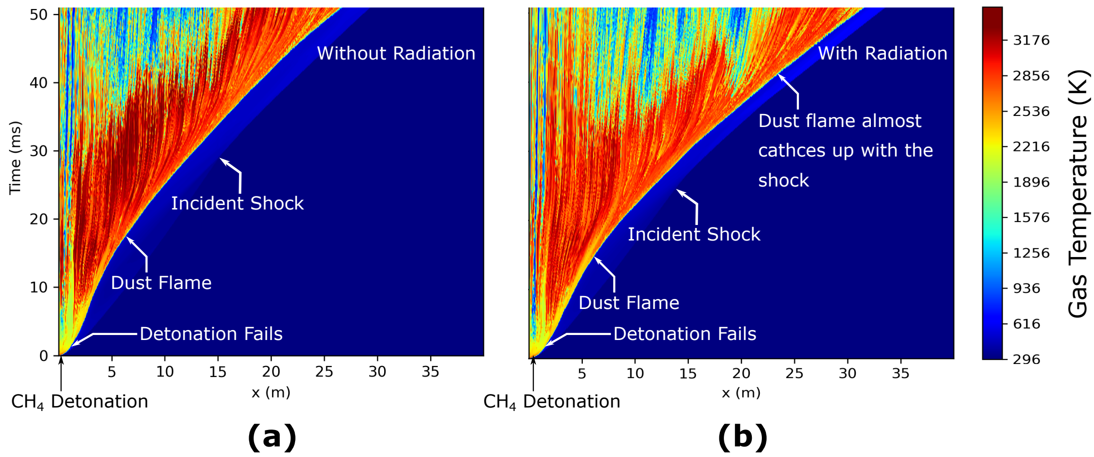

Figure 2: X-t diagram for the 40-m long channel with 30 μm particles shaded by gas phase temperature at y = 5 cm (a) without radiation and (b) with radiation.

3 Results and Discussion

Figure 2 shows position-time (X-t) diagrams for the long channel case with 30 μm particles at y = 5 cm. At very early times a CH_4 detonation is ignited and propagated to the right. The detonation fails at $\sim$0.5 ms and the flame and shock fronts separate. The shock keeps traveling right which disperses the coal dust into the air. The flame follows the shock, initially decelerating and then accelerating after $\sim$8 ms. After the detonation fails, the remaining pre-suspended methane-air mixture continues to ignite along with the shock-dispersed coal dust. Once the methane-air mixture is completely consumed, the coal dust sustains the flame propagation.

Figure 3 shows the flame locations, shock locations, and the total chemical heat release rates for both the radiative and non-radiative cases in (a) 40-m long channel, and (b) the shorter 10-m channel. In Figure 3 (a), we observe that initially the shock and flame velocities for the radiative case are slightly higher than the non-radiative case for most of the simulations. As the flame keeps propagating, the peak chemical heat release rates for the radiative is about 60 GW/m higher than the non-radiative cases at $\sim$32 ms. The flame and shock fronts also accelerate more than the non-radiative case. Towards the end of the simulation at $\sim$56 ms, the radiative flame front is catching up to the leading shock. It is possible that if the channel was longer and the simulation was run for more time, this dust flame could transition to a quasidetonation. The flame speeds at this time are about 1 km/s, which is close to the quasidetonation wave velocity of 1.5 km/s for coal dusts [14]. This is also seen for the non-radiative case, although the acceleration and transition to quasidetonative state appears to occur earlier for the radiative case.

In Figure 3 (b), we observe only minor differences between the radiative and non-radiative cases in the shorter 10-m channel which we have studied earlier [2]. Both the shock and the flame for the radiative case are slightly ahead of the non-radiative case. The heat release rate is the same as the non-radiative case for the most part. During the detonation, the heat release rate is $\sim$0.5 GW/m for both cases, then climbs to over 100 GW/m. The heat release rate drops significantly at $\sim$25 ms, which is when the reflected shock interacts with the flame. This process is detailed in [2].

Figures 4 and 5 compare the gauge pressure and the impulse, respectively, between the radiative and non-radiative cases for gauges that are placed at 1 m, 6 m, and 10 m for the short channel, and 1 m, 10 m, 20 m, and 30 m for the long channel at a height of 2.5 cm in the channel. The gauge pressures for the radiative case are significantly higher than those for the non-radiative case. As the shock travels through

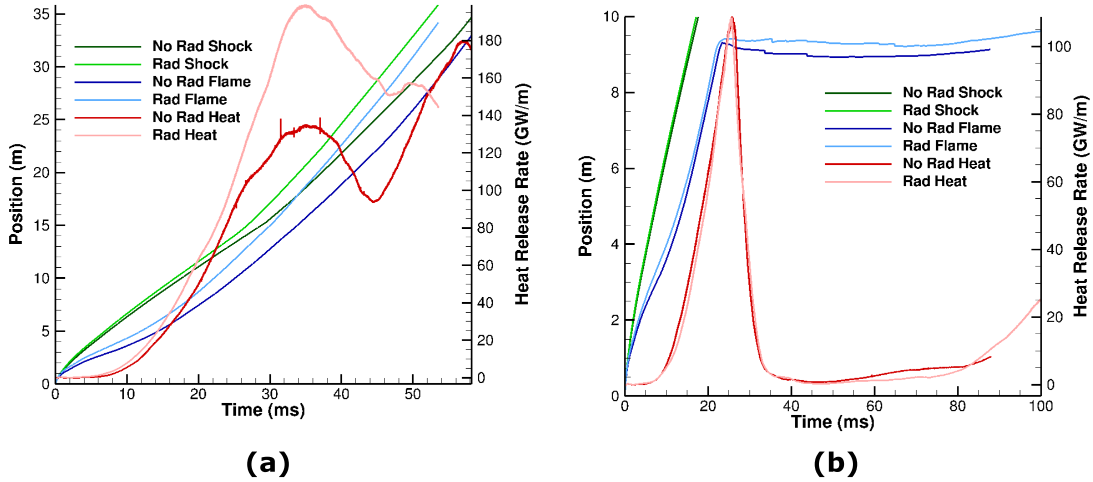

Figure 3: Shock and flame positions and heat release rates due to chemical reactions with 30 μm particles for the (a) 40-m channel and (b) 10-m channel.

these locations, there is a step-change in the pressure. This higher post-shock pressure then falls sharply for the gauge at 1 m due to the Taylor following the detonation. The Taylor wave weakens and has little influence on the pressure-time traces beyond 1 m. The peak pressures at at these gauges reach values that are higher than the post-shock pressure, indicating that the dust explosion is much more damaging than the leading shock. A similar situation is revealed by the impulse plots in Figure 5. In the radiative case, the impulse values are observed to be more than 10 kNs higher than the non-radiative case towards the end of the simulation. Both the overpressure and impulse plots for the long channels show that the flame and shock fronts for the radiative case are ahead of the non-radiative case and the difference grows with time, reiterating that the radiative flame accelerates faster than the non-radiative case.

4 Conclusions

Layered coal-dust explosions were simulated using computational methods. Several scenarios were investigated both with and without radiation heat transfer. Two different channel lengths of 10 m and 40 m were considered - the first one to see how the reflected shock affects the flame propagation, and the second to check how the flame progresses unhindered. These two-dimensional simulations also considered 30 μm particles which have the highest explosibility.

The simulation results show that vital flame parameters, such as flame temperature, velocity, and structure, are often substantially different for the cases considering radiation compared to those that neglect radiation. Due to the complex and non-linear behavior of radiation, the influence it has on these parameters can however be opposite, as observed in our previous studies. In the cases outlined in this study, radiation increased the combustion rate and accelerated the flames by the process of pre-heating the particles. This in turn increases the severity of the explosion. As seen with the radiative cases, the gauge pressure and impulse values are considerably higher than the non-radiative cases which shows the importance of including thermal radiation in dust explosion simulations. These differences become more evident in the 40-m long channel cases since the dust flame is allowed to propagate unhindered, unlike in the short 10-m channel cases where the reflected shock interaction with flame limits the flame propagation. Ongoing work is examining the effects of detailed chemistry models and a spectrally accurate radiation model.

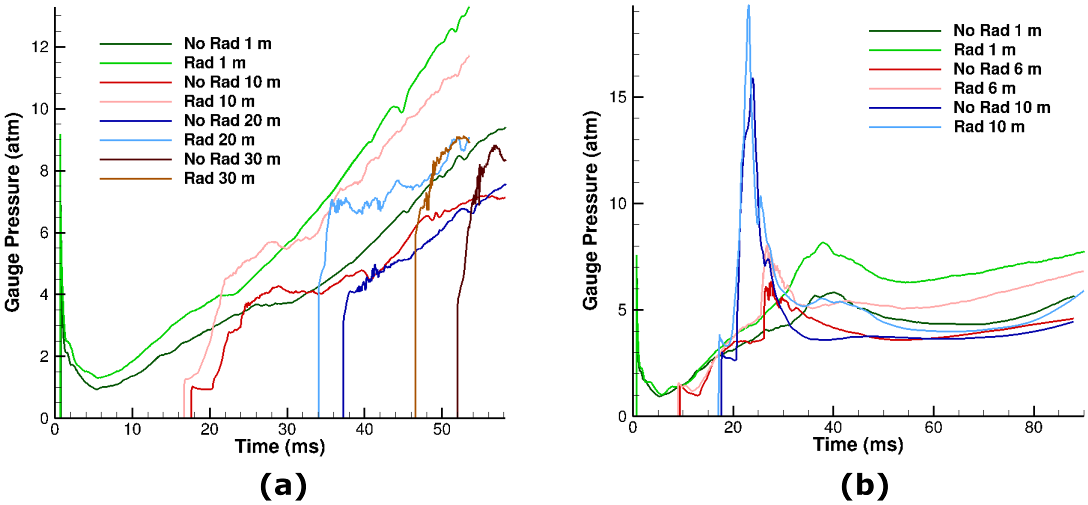

Figure 4: Gauge pressure plots for the (a) 40-m channel at locations of 1 m, 10 m, 20 m and 30 m; and (b) 10-m channel at locations of 1 m, 6 m and 10 m in the channel, and at a height of 2.5 cm in the channel. Both radiative and non-radiative cases with 30 μm particles are shown.

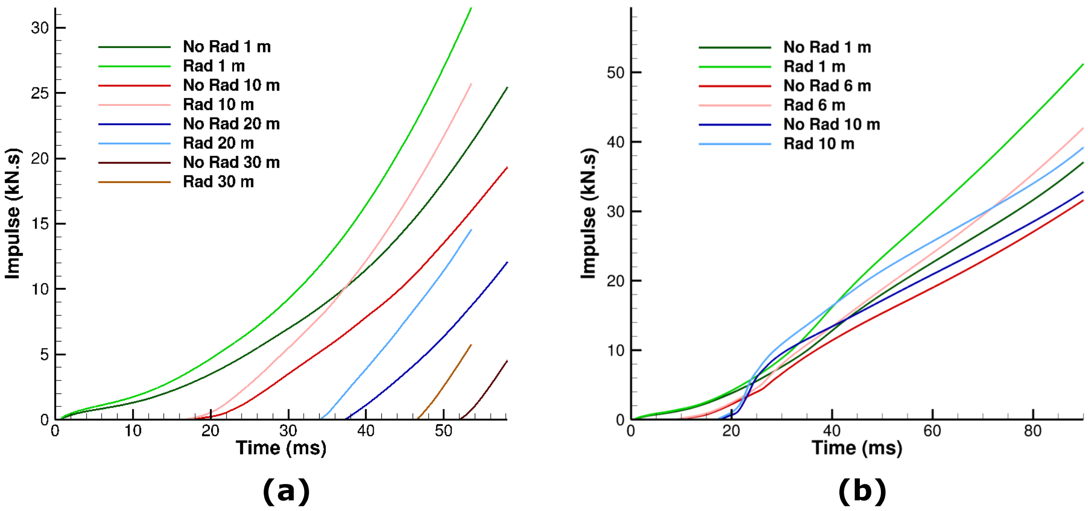

Figure 5: Impulse plots for the (a) 40-m channel at locations of 1 m, 10 m, 20 m and 30 m; and (b) 10-m channel at locations of 1 m, 6 m and 10 m in the channel, and at a height of 2.5 cm in the channel. Both radiative and non-radiative cases with 30 μm particles are shown.

5 Acknowledgements

This work was supported in part by the US National Science Foundation (NSF) grant 1942861. The calculations presented in this paper were performed using the University of Florida high-performance computing cluster, HiPerGator.

References

[1] Guhathakurta, S., & Houim, R. W. (2021). Influence of thermal radiation on layered dust explosions. Journal of Loss Prevention in the Process Industries, 72, 104509.

[2] Guhathakurta, S., & Houim, R. W. (2022). Impact of particle diameter and thermal radiation on the explosion of dust layers. Proceedings of the Combustion Institute.

[3] Cashdollar, K. L. (2000). Overview of dust explosibility characteristics. Journal of loss prevention in the process industries, 13(3-5), 183-199.

[4] Houim, R. W., & Oran, E. S. (2015). Numerical simulation of dilute and dense layered coal-dust explosions. Proceedings of the Combustion Institute, 35(2), 2083-2090.

[5] Houim, R. W., & Oran, E. S. (2016). A multiphase model for compressible granular–gaseous flows: formulation and initial tests. Journal of fluid mechanics, 789, 166-220.

[6] Houim, R. W., & Kuo, K. K. (2011). A low-dissipation and time-accurate method for compressible multi-component flow with variable specific heat ratios. Journal of Computational Physics, 230(23), 8527-8553.

[7] Radice, D., Abdikamalov, E., Rezzolla, L., & Ott, C. D. (2013). A new spherical harmonics scheme for multi-dimensional radiation transport I. Static matter configurations. Journal of Computational Physics, 242, 648-669.

[8] Grosshandler, W. L. (1993). RADCAL: a narrow band model for radiation. Calculations in a Combustion Environment, NIST Technical Note, 1402.

[9] Buckius, R. O., & Hwang, D. C. (1980). Radiation properties for polydispersions: application to coal.

[10] Franzelli, B., Riber, E., Gicquel, L. Y., & Poinsot, T. (2012). Large eddy simulation of combustion instabilities in a lean partially premixed swirled flame. Combustion and flame, 159(2), 621-637.

[11] Kobayashi, H., Howard, J. B., & Sarofim, A. F. (1977, January). Coal devolatilization at high temperatures. In Symposium (international) on combustion (Vol. 16, No. 1, pp. 411-425). Elsevier.

[12] Baek, S. W., Sichel, M., Kauffman, C. W. (1990). Asymptotic analysis of the shock wave ignition of dust particles. Combustion and flame, 81(3-4), 219-228.

[13] Bradley, D., Lawes, M., Park, H. Y., Usta, N. (2006). Modeling of laminar pulverized coal flames with speciated devolatilization and comparisons with experiments. Combustion and flame, 144(1-2), 190-204.

[14] Edwards, D. H., Fearnley, P. J., & Nettleton, M. A. (1987). Detonation limits of clouds of coal dust in mixtures of oxygen and nitrogen. Combustion, Explosion and Shock Waves, 23(2), 239-245.